Zeolite Membrane Synthesized Employing Crystal Growth Inhibitors for Carbon Dioxide Separation

*Surendar R.Venna and Moises A. Carreon**
University of Louisville, Department of Chemical Engineering, Louisville, KY-40292, USA.

*Corresponding author: macarr15@louisville.edu

Introduction

Silicoaluminophosphate molecular sieves have been the subject of great interest because of their high thermal resistance, mechanical strength, chemical stability, chemical inertness, and uniform-sized pores of molecular dimensions. SAPO-34 with the composition of $Si_xAl_yP_zO_2$ (x = 0.01-0.98, y = 0.01-0.6 & z = 0.01-0.52) is a representative type of silicoaluminophosphate zeolite displaying chabazite structure with uniform microporous channels and cages. SAPO-34 an acid silico-aluminophosphate zeolite with pore size of ~0.38nm, posses unique shape selectivity, which is of great interest in the field of gas separation (in particular in the separation of carbon dioxide from different light gases) and heterogeneous catalysis (in particular especially in methanol-to-olefin reaction in petrochemical industries). Small zeolite crystals are preferred because they display more improved surface properties compared to larger particles. For smaller crystals more number of atoms are exposed to the surface increasing the acidity, which results in higher selectivity when SAPO-34 is used for methanol to olefin reactions (1, 2). Smaller crystals potentially result in thinner membranes which lead to improved separation performance (3, 4).

Lok and co-workers at Union Carbide first reported the synthesis of SAPO-34 in 1984 (5). Later, various routes for the preparation of SAPO-34 have been proposed. SAPO-34 has been synthesized by using TEAOH (6), TEAOH along with DPA (3), different templates (7, 8, 9), via vapor phase transport (10), various sources of silica and alumina (11). Also, the incorporation of different metals in SAPO-34 framework like Mg, Ca, Ti, Ag, Na, Sr, Ce (12) and Cu, Co (13) has been done. SAPO-34 has been used in various functional applications such as separation of carbon dioxide from different gases (4, 14), catalyst for methanol to olefin reactions (1, 2), H_2 purification and storage (15), chloromethane transformation to higher hydrocarbons (16), as a hydrocarbon trap (17).

Here, we present the synthesis of SAPO-34 crystals using various crystal growth inhibitors (polyethylene glycol, polyoxyethylene lauryl ether and methylene blue) and several structure directing agents (tetraethylammonium hydroxide, dipropylamine, morpholine and triethyl amine). The resultant SAPO-34 crystals were characterized by BET, XRD, SEM, FTIR, TGA and CO_2/CH_4 adsorption. The surface area of the SAPO-34 crystals increased as compared to the samples synthesized without crystal growth inhibitors. The crystallinity of SAPO-34 was confirmed by XRD and FTIR. The CO_2 and CH_4 adsorption capacity of SAPO-34 was studied.

Experimental

$Al(i\text{-}C_3H_7O)_3$ (> 99.99%, Aldrich), H_3PO_4 (85 wt% aqueous solution, Aldrich) and Ludox (40 wt%, Aldrich) were used as the inorganic precursors. Tetraethyl ammonium hydroxide and dipropylamine (99wt%, Aldrich) were used as templates. Polyethylene glycol-600 (PEG, Alfa Aesar),pPolyoxyethylene lauryl ether (C12E6, Acros Organics) and methylene blue (MB, Sigma-Aldrich) were used as crystal growth inhibitors (CGI). The composition of the synthesis gel was $1Al_2O_3$:$1H_3PO_4$:$0.3SiO_2$:1TEAOH:1.6DPA:$77H_2O$: xCGI, where x is in the range of 0.037-0.175. $Al(i\text{-}C_3H_7O)_3$ and H_3PO_4 were mixed with distilled H_2O for 2hrs. Then, ludox was added and the resulting solution was stirred for additional 2hrs to form a homogeneous solution. Then the templates TEAOH and DPA were added to the gel with an interval of 30 min. After stirring for 30 min, crystal growth inhibitors were added. The resulting gel was aged for 3 days at 50^0C. It was transferred to a stainless steel autoclave and hydrothermal treatment was done using a conventional oven at 220^0C for 24 hrs. The hydrothermal treatment was also done with controlled temperature ramp (i.e. increasing 1^0C/min till125^0C and hold there for 5hrs and then increasing the temperature to 220^0C at 1^0C/min and hold there for 16hrs). The solution after the hydrothermal treatment was centrifuged at 4000rpm for 20min to separate the seeds from the mother liquor. The resultant seeds were dried overnight at 60^0C. The templates and CGI were removed at 550^0C for 5hrs with heating and cooling rates of 1^0 and 10^0C/min respectively. The calcined SAPO-34 samples were characterized using FE-SEM (FEI Nova 600) to study the size and morphology. Brukar D8 Discover XRD and Spectrum BX FTIR (Perkin Elmer) were used to determine the crystal structure and functional groups at the SAPO-34 surface, respectively. Micromeritics Tristar-3000 model BET porosimeter was used to study the surface area measurements and CO_2/CH_4 adsorption ratios.

Results and Discussion

A typical X-ray diffraction of the SAPO-34 crystals synthesized with MB as CGI is shown in Figure 1. The spectrum shows the chabazite structure confirming the presence of pure SAPO-34 crystals. The position of each peak is identical to those reported for SAPO-34 (6). The synthesized samples were also characterized by the Fourier transform IR to confirm the formation of SAPO-34. A typical FTIR spectrum is shown in Figure 2 for the sample synthesized using PEG as the crystal growth inhibitor. The lattice vibrations in the framework of SAPO-34 crystals are typical for the chabazite framework which is in agreement with previous reported data (18). The most prominent IR band of the SAPO-34 frameworks occurs in the region between 900 and 1300 cm^{-1}, which is asymmetric stretching of AlO_4^{-1}, and PO_4^{-1} tetrahedra. The other peaks corresponding to SiO_4^{-1} bonding, vibrations in the double bond region and -OH bonding are weaker bands in the 400-500, 600-700 and 1600-1700 cm^{-1} region. Therefore, XRD and FTIR confirm the formation of pure SAPO-34 using crystal growth inhibitors.

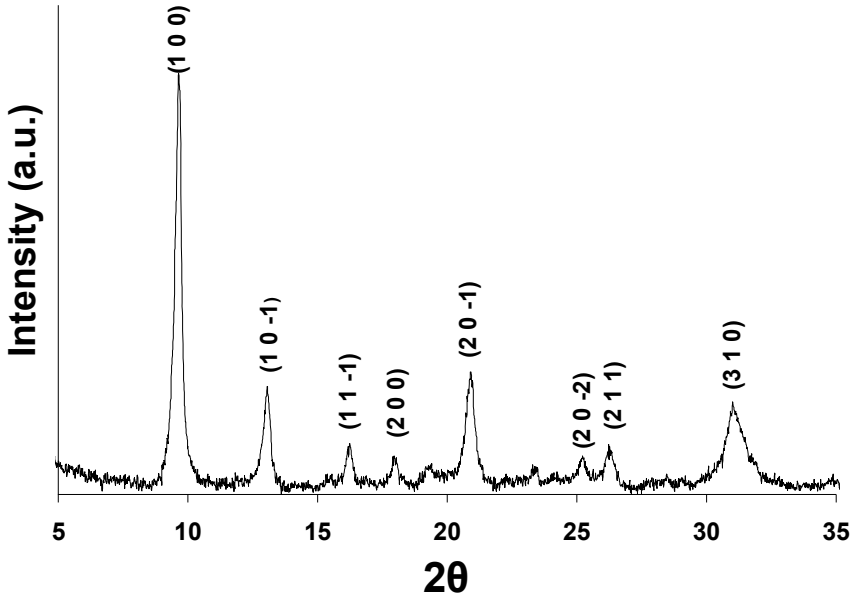

Figure 1: XRD pattern of the chabazite structure synthesized using MB as crystal growth inhibitor

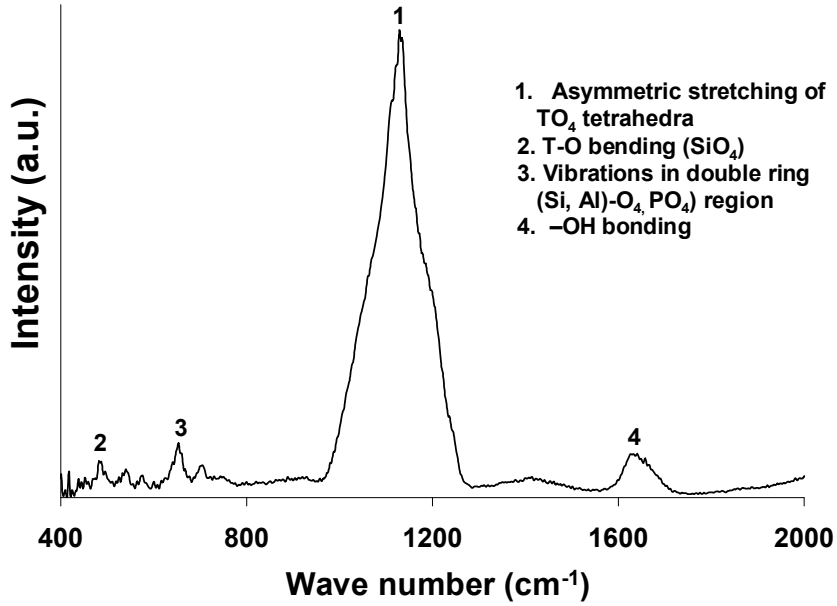

Figure 2: FTIR spectra of SAPO-34 crystals synthesized using PEG as crystal growth inhibitor

SEM images showing the cubic and rhombohedral crystals of SAPO-34 synthesized using the crystal growth inhibitors and ramp heating are shown in Figure 3. The incorporation of crystal growth inhibitors during synthesis led to a remarkable decrease in

crystal size from ~2 μm to ~0.5 μm. In general, crystal sizes between ~0.5-1 μm were obtained for samples prepared with crystal growth inhibitors. Crystal growth inhibitors play an important role in changing the alkalinity of the synthesis of gel, which helps to form smaller nuclei and therefore smaller crystals (19). They also interact with reactive sites of the precursors suppressing the crystal growth. They may also adsorb on to the surface of the nuclei to prevent the growth (20).

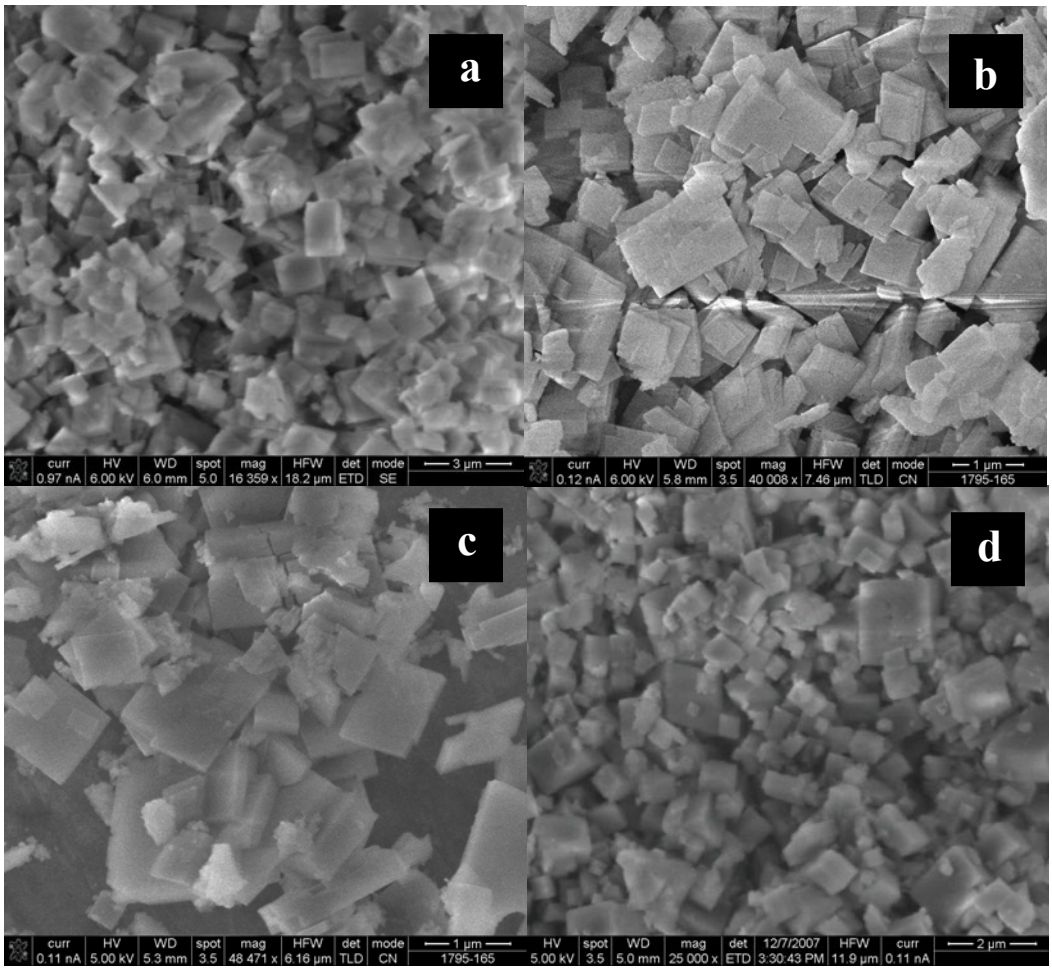

Figure 3: SEM images of the SAPO-34 crystals synthesized employing a) PEG, b) C12E6, and c) MB as crystal growth inhibitors and d) without crystal growth inhibitors

Nitrogen adsorption isotherms at 77 K were used to determine the BET surface area of SAPO-34 crystals. The surface areas of the different samples synthesized using the crystal growth inhibitors are shown in Figure 4. Surface Area of SAPO-34 crystals significantly increased about 25% - 80%. For example areas up to ~700 m^2/g were obtained when C12E6 was employed as CGI, while surface areas in the range of only ~390 m^2/g to ~500 m^2/g were observed for the samples synthesized without any CGI.

The higher surface areas obtained using crystal growth inhibitors are assumed to be a result of the formation more nuclei during the initial stages of hydrothermal synthesis and controlled the growth of the crystals in later stages.

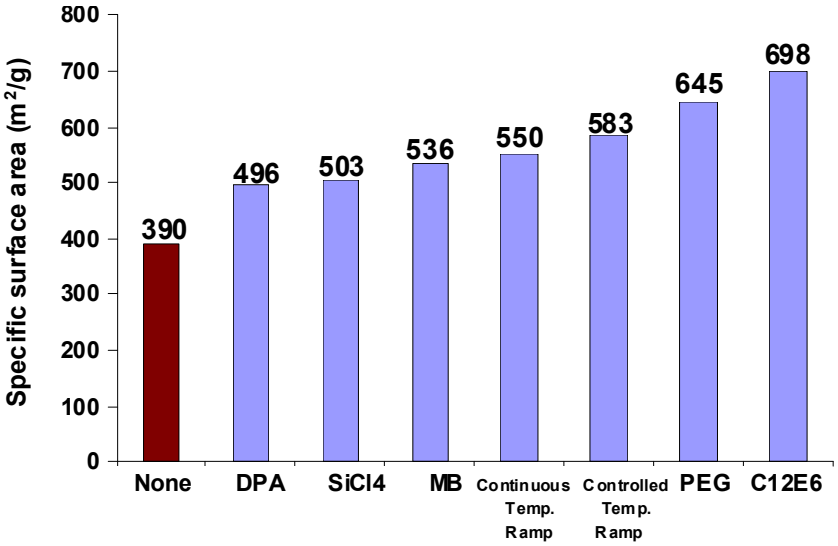

Figure 4: BET surface area of SAPO-34 crystals synthesized using different crystal growth inhibitors and controlled temperature ramp

CO_2 and CH_4 adsorption capacity of SAPO-34 crystals was conducted at room temperature using water the coolant. The CO_2/CH_4 adsorption capacity of the SAPO-34 samples synthesized with different CGI is much higher (~9) than the samples synthesized without growth inhibitors (~5). Typical CO_2 and CH_4 adsorption isotherms are shown in Figure 5 for a SAPO-34 sample synthesized employing C12E6 as the crystal growth inhibitor. The higher adsorption capacity of the samples synthesized using CGI is due to the incorporation of more nitrogen in the framework of SAPO-34, as confirmed by CHN analysis (not shown here).

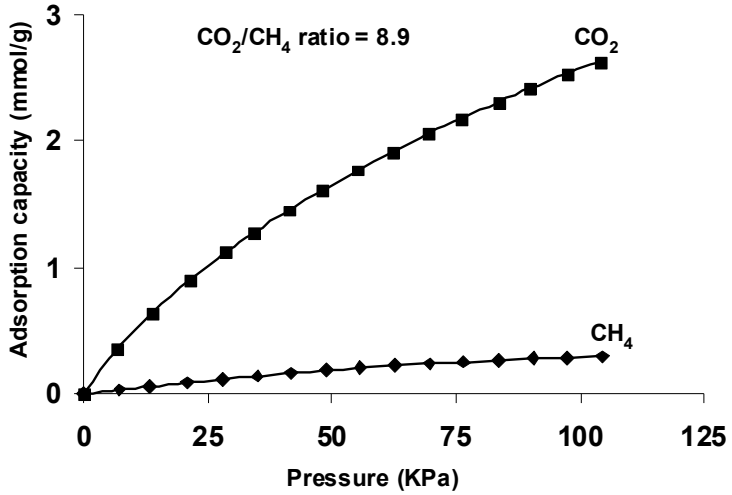

Figure 5: CO_2/CH_4 adsorption capacity of SAPO-34 crystals synthesized using C12E6 as CGI

The synthesized SAPO-34 crystals can be potentially used as *seeds* to prepare thin membranes on porous supports to separate the CO_2 from CH_4. In addition to their chemical and thermal stability, SAPO-34 is attractive as membrane material because of their atomically ordered nanometer-scale pore structures. SAPO-34 also, can be potentially used as catalysts in the methanol to olefins reaction because of its high surface area, and moderate acidity with more active sites exposed to reactants.

Conclusions

- SAPO-34 crystals were synthesized employing crystal growth inhibitors.
- XRD and FTIR confirmed the presence of chabazite structure of typical SAPO-34
- Crystal growth inhibitors (Poly ethylene glycol, polyoxyethylene lauryl ether and Methylene blue) reduced the crystal size and increased the specific surface area of SAPO-34 crystals.
- SAPO-34 crystals (~0.5-1 μm) displaying BET surface areas up to ~700m^2/g were prepared.
- The carbon dioxide adsorption capacity of SAPO-34 increased with the incorporation of crystal growth inhibitors
- Controlled two-stage hydrothermal heating method led to high surface area crystals with narrow size distribution.

References

1. S Y.J. Lee, S.C. Baek, K.W. Jun, (2007), *Appl. Catalysis A: General*, *329*, 130–136
2. M. Popova, Ch. Minchev, V. Kanazirev, (1998), *Appl. Cat. A: General, 169*, 227-235
3. S. Li, J.L. Falconer, R.D. Noble, (2008), *Micro. Meso. Mater. 110*, 310-317.
4. M.A. Carreon, S. Li, J.L. Falconer, R.D. Noble, (2008), *J. Am. Chem. Soc. 130*, 5412–5413
5. B. M. Lok, C. A. Messina, R. L. Patton, R. T. Gajek, T. R. Cannan, E. M. Flanigen, (1984), *J. Am. Chem. Soc. 106*, 6092-6093
6. H. V. Heyden, S. Mintova, T. Bein, (2008)*, Chem. Mater. 20,* 2956-296.
7. Ø. B. Vistad, D. E. Akporiaye, F. Taulelle, K. P. Lillerud, (2003), *Chem. Mater. 15,* 1639-1649
8. E. Dumitriua, A. Azzouz, V. Hulea, D. Lutic, H. Kessler, (1997), *Micro. Mater. 10*, 1-12.
9. G. Liu, P. Tian, Y. Zhang, J. Li, L. Xu, S. Meng, Z. Liu, (2008), *Micro. Meso. Mater.* 114, 416-423
10. J. Yao, H. Wang, S. P. Ringer, K.Y. Chan, L. Zhang, N. Xu, (2005), *Micro. Meso. Mater. 85*, 267-272
11. M. Mertens, K. G. Strohmaier, (2004), *U.S. Patent 6696032 B2*.
12. M. E. Rivera-Ramos, G. J. Ruiz-Mercado, A. J. Herna´ndez-Maldonado, (2008), *Ind. Eng. Chem. Res. 47,* 5602–5610

13. E. L. Uzunova, H. Mikosch, J. Hafner, (2008), *J. Phys. Chem. C. 112,* 2632-2639
14. J.C. Poshusta, V.A. Tuan, E.A. Pape, R.D. Noble, J.L. Falconer, (2000), *AIChE J. 46*, 779-789
15. M. Yu, S. Li, J.L. Falconer, R.D. Noble, (2008), *Micro. Meso. Mater. 110*, 579-582
16. Y. Wei, D. Zhang , Z. Liu, B. L. Su, (2007), *Chemical Physics Letters*, 444, 197–201
17. S.P. Elangovan, M. Ogura, Y. Zhang, N. Chino, T. Okubo, (2005), *Appl. Cat. B: Environ. 57*, 31–36
18. D. B. Akolekar, S. Bhargava, W. V. Bronswijk, (1999), *Applied spectroscopy*, 53, 931-937
19. H. Hosokawa, K. Oki, (2003), *Chemistry Letters,* 32, 586-587
20. C.M. Lew, Z. Li, S. I. Zones, M. Sun, Y.Yan, (2007), *Micro. Meso. Mater.* 105, 10-14